ELSEVIER

NeuroImage

www.elsevier.com/locate/ynimg
NeuroImage 37 (2007) 561–571

Localizing pre-attentive auditory memory-based comparison: Magnetic mismatch negativity to pitch change

Burkhard Maess,[a,*] Thomas Jacobsen,[b] Erich Schröger,[b] and Angela D. Friederici[a]

[a]*Max Planck Institute of Human Cognitive and Brain Science, Stephanstr. 1a, D-04104 Leipzig, Germany*
[b]*Institute of Psychology I, University of Leipzig, Germany*

Received 23 February 2007; revised 25 April 2007; accepted 11 May 2007
Available online 2 June 2007

Changes in the pitch of repetitive sounds elicit the mismatch negativity (MMN) of the event-related brain potential (ERP). There exist two alternative accounts for this index of automatic change detection: (1) A sensorial, non-comparator account according to which ERPs in oddball sequences are affected by differential refractory states of frequency-specific afferent cortical neurons. (2) A cognitive, comparator account stating that MMN reflects the outcome of a memory comparison between a neuronal model of the frequently presented standard sound with the sensory memory representation of the changed sound. Using a condition controlling for refractoriness effects, the two contributions to MMN can be disentangled. The present study used whole-head MEG to further elucidate the sensorial and cognitive contributions to frequency MMN. Results replicated ERP findings that MMN to pitch change is a compound of the activity of a sensorial, non-comparator mechanism and a cognitive, comparator mechanism which could be separated in time. The sensorial part of frequency MMN consisting of spatially dipolar patterns was maximal in the late N1 range (105–125 ms), while the cognitive part peaked in the late MMN-range (170–200 ms). Spatial principal component analyses revealed that the early part of the traditionally measured MMN (deviant minus standard) is mainly due to the sensorial mechanism while the later mainly due to the cognitive mechanism. Inverse modeling revealed sources for both MMN contributions in the gyrus temporales transversus, bilaterally. These MEG results suggest temporally distinct but spatially overlapping activities of non-comparator-based and comparator-based mechanisms of automatic frequency change detection in auditory cortex.

Keywords: Mismatch negativity (MMN); N1; Change detection; Sound frequency; Pitch; Auditory sensory memory; Magnetoencephalography (MEG); Equivalent current dipole

Introduction

During auditory processing, the discrimination of pitch is vital, not only for the perception of speech and music but also for the recognition of auditory objects in general. The human auditory system is able to detect changes in pitch already during early infancy and even before birth (e.g., Huotilainen et al., 2005; Weber et al., 2004).

When auditory stimuli of equal pitch are sequentially presented, deviations from this uniform pitch are pre-attentively detected. This pitch change detection process is reflected by the mismatch negativity (MMN) of the event-related brain potential (ERP) (e.g., Näätänen et al., 1978). Typically, MMN to pitch has been investigated by comparing ERPs to standard and deviant stimuli presented in a so-called oddball block consisting of frequently occurring standards and rarely occurring deviants (e.g., Näätänen et al., 1989; Paavilainen et al., 1991). For a wide range of stimuli, there is evidence that the MMN is elicited if a comparison process, based on auditory sensory memory, leads to a detection of a discrepancy between the representation of a regularity inherent in recent stimulation and the representation of a current deviant stimulus (e.g., Näätänen et al., 2001). That is, the MMN is taken to reflect the operation of a pre-attentive memory-based comparison mechanism (e.g., Näätänen, 1992; Winkler et al., 1993; for reviews, see Näätänen et al., 2005; Kujala et al., 2007).

An alternative hypothesis regarding the generation of the MMN is based on the assumption that there are frequency-specific afferent cortical neural populations. Frequency processing is based on the tonotopic organization of the auditory system which is preserved from the cochlea throughout the cortex (e.g., Pantev et al., 1988; Romani et al., 1982). Stimulus repetition leads to repeated initiation of patterns of activity in the same neural population leading to an attenuation of the exogenous ERPs (e.g., the N1) with stimulus repetition (e.g., Butler et al., 1969; Picton et al., 1978; Näätänen et al., 1988). In accordance with Ritter et al. (1968) and Näätänen (1992), this attenuation is interpreted in terms of neural refractoriness rather than habituation because no dishabituation was demonstrated (Näätänen and Picton, 1987). Thus, in oddball blocks,

* Corresponding author. Fax: +49 3425 887511.
E-mail address: maess@cbs.mpg.de (B. Maess).
Available online on ScienceDirect (www.sciencedirect.com).

1053-8119/$ - see front matter © 2007 Elsevier Inc. All rights reserved.
doi:10.1016/j.neuroimage.2007.05.040

the differing probabilities of stimulus occurrence may lead to different refractory states of those subpopulations of neurons that are either activated by the standard or by the deviant, but not by both. The neural response elicited by standard stimuli is therefore suppressed more by these refractory effects than the response to the less frequent deviant stimuli. Consequently, the traditional procedure that uses physically different standards and deviants from the same block might misestimate an MMN contribution reflecting automatic sensory memory processes, because of such differential states of refractoriness of respectively recruited neural populations (cf. e.g., Jääskeläinen et al., 2004; Kujala et al., 2007; Näätänen et al., 2005; Näätänen and Alho, 1997; Schröger, 1997). Therefore, under the assumption of frequency-specific cortical neurons, the brain could detect changes in sound frequency on the basis of differential neural refractory states (or different patterns of neural activation in general), and not on the basis of a comparison mechanism relying on auditory sensory memory. Thus, the one account for frequency MMN is more sensorial in nature and reflects a non-comparator mechanism of automatic change detection, whereas the other is more cognitive reflecting a comparator mechanisms involving memory representations (for a related distinction of mechanisms of the orienting response, cf. Siddle, 1991).

By applying appropriate control conditions, one may be able to disentangle non-comparator-based and comparator-based contributions to MMN. Such control conditions have been utilized by Jacobsen and Schröger (2001) in a recent ERP experiment, in which the stimulus set includes several sound exemplars varying along the frequency dimension. For example, a 500-Hz tone served as a deviant amongst 550 Hz standard tones in the oddball block (deviant probability being 10%); the same tone was also presented in a control block together with nine other tones differing in frequency (550, 605, 666, 732, 805, 886, 974, 1072 and 1179 Hz). Therefore, neurons tuned to frequencies of about 500 Hz will not have a higher degree of refractoriness in the control condition than in the oddball condition since they are presented with the same probability as the physically identical tones serving as deviants in the oddball condition. This manipulation prevents the contribution of the relative increase of N1 elicited by deviant stimuli to the MMN. The ERP results supported the hypothesis of an N1 refractoriness contribution to the early time range of MMN and a memory comparison based in the late time range of MMN.

This approach has been successfully applied to MMN elicited by different stimulus dimensions (Schröger and Wolff, 1996; Jacobsen and Schröger, 2003; Jacobsen et al., 2003a). Recently, an fMRI study following this approach has been conducted (Opitz et al., 2005). It revealed neural activities for the change versus control (comparator part) and for the control versus standard (non-comparator part) contrasts, which were localized in auditory cortex. However, due to the temporal constraints of fMRI, these contributions could not be separated in time. Moreover, as changes in oddball paradigms often evoke later effects (P3a), the identified generators might contain P3a contribution as well. The present study used whole-head MEG to further elucidate the temporal and structural characteristics of the sensorial and cognitive contributions to frequency MMN. MEG is an important tool in exploring the mechanisms of auditory deviance detection, providing assessments of its mental chronometry as well as neural source localizations. Earlier MEG studies of the MMN identified sources in auditory cortex (e.g., Alho et al., 1993; Korzyukov et al., 2003; Rinne et al., 2000; Tiitinen et al., 1993; Tervaniemi et al., 1999; for a review, see Alho, 1995). As MMN to changes in sound frequency has become very widely used in basic and applied research as well as applications proper (e.g., Fischer et al., 1999; Pekkonen et al., 2001), a more elaborated view concerning the generation of the frequency MMN is required. In pathological cases of an impaired MMN, it would be important to know whether the impairment is related to the sensorial or the cognitive contribution to MMN.

For the present study on sound frequency processing, it was predicted that genuine magnetic MMN (MMNm) to changes in sound frequency would be obtained, as well as MMNms derivable in the traditional way by deviant-minus-standard subtractions. The chronometric properties of these evoked magnetic difference fields were expected to conform to the time courses obtained with the EEG measurements. Furthermore, the traditional MMN was expected to show a monophasic temporal pattern of the difference fields corresponding to a negativity in ERP data. Contrary to this pattern, the deviant-minus-control comparison was predicted to reveal a biphasic temporal pattern consisting of a reverse effect in the N1 latency range followed by a genuine memory-comparison-based MMNm. With spatial principal component analyses the 148-channel data shall be mapped into a small number of virtual channels. We predict that the variance of the data can be accounted for by one or two factors because we expect to find one or two pairs of activated regions. Finally, we wanted to localize the sources of the respective contributions to automatic change detection in the N1 and in the MMN range in order to assess whether these can be separated not only in time but also in space. As grand-average event-related fields (ERFs) are not optimal for source localizations (Lütkenhöner, 2003), we generated volume conductor models based on individual magnetic resonance images (MRIs) to determine the neural generators of the change-related ERFs. In every individual participant, sources of the non-comparator and comparator-based contribution to automatic change detection should localize to coordinates in auditory cortices, when models are used that fit one moving dipole per hemisphere in each condition. According to MEG results based on grand-average ERFs which localized N1 and MMN in slightly separate auditory areas, one might expect spatially distinctive sources also for the non-comparator and comparator contributions of MMN (e.g., Jääskeläinen et al., 2004; Korzyukov et al., 2003).

Materials and methods

Participants

Fifteen volunteers participated in the study (9 male, 6 female). The mean age was 23.6 years (median 24; range 22 to 31). Participants were right-handed (Laterality quotient >90 according to Oldfield, 1971) and reported normal auditory and normal or corrected-to-normal visual acuity. They gave informed consent and received monetary compensation. Three additional participants had to be excluded from further analysis due to above threshold head movements.

Stimuli

Ten sinusoidal tones of 500, 550, 605, 666, 732, 805, 886, 974, 1072 and 1179 Hz were used (cf. Jacobsen and Schröger, 2001). They comprised a tonal succession with a 10% increment in frequency starting at 500 Hz. Tones were 50 ms long including 5 ms rise and 5 ms fall times. In addition, a selection of silenced movies was used.

Apparatus

Acoustical stimuli were administered via a Soundblaster SB16 sound board and 4D-Neuroimaging sound transmissions system. Sound pressure level was calibrated using an artificial head (HeadAcoustics HMSIII digital). The experiment was run in a magnetically shielded experimental chamber (Vakuumschmelze Hanau). MEG was recorded with a whole-head WHS2500 (4D-Neuroimaging). Off-line signal processing was carried out using EEP 3.0 (MPI-CNS; ANT Software), Curry 4.5 (NeuroScan) and SAS 8.02.

Procedure

The participants were seated (12) on a comfortable chair or were supine on a bed. They were instructed to watch a self-selected silenced movie without subtitles on a 17-in. projection screen positioned approximately 80 cm in front of them and to ignore the auditory stimulation. Tones were sequentially presented binaurally over ear plugs at a sound pressure level (SPL) of 73 dB with a stimulus onset-to-onset interval of 500 ms. There were three blocked conditions, (a) descending deviant (500 Hz) with a 550-Hz standard, (b) ascending deviant (1179 Hz) with a 1072-Hz standard and (c) control comprised of all ten tones. The block design is shown in Fig. 1. Each block was presented twice within one session. Two sessions were conducted with at least 7 days between them. Block sequence was counterbalanced across participants. Each block consisted of 1500 trials. In oddball blocks, deviants occurred among standards with a relative frequency of 0.1 in a pseudorandomized fashion with the constraint that two deviants could not be directly repeated. deviants came from the endpoints of the tonal succession, the standards being their closest neighbors. In the control block, stimuli were presented equiprobably (relative frequency = 0.1) in a pseudorandomized sequence such that the set of ten tones was multiply presented in sequence—each in random order while repetitions of tones were avoided. This procedure resulted in physically identical tones being used as controls, presented in the control block, as well as deviants, presented in the oddball blocks, each showing an equal frequency of occurrence within a block. Thus, the only difference between both presentations was that neurons specifically responding to the sound frequency of controls/deviants were less refractory for controls than for deviants because they were presented among nine other control stimuli showing a larger frequency separation in the control block, than the standard–deviant separation in the oddball block (cf. also Jacobsen et al., 2003a,b). An experimental session lasted approximately 3 h including preparation of the participant, data acquisition, breaks and post-experimental procedures.

Magnetic and electrophysiological recordings

The magnetoencephalogram (MEG) was recorded continuously from 148 magnetometer channels. Electroocular activity (EOG) was monitored by two bipolar channels. The vertical EOG was recorded from the right eye by supra- and infraorbital electrodes. The horizontal EOG was recorded from electrodes lateral to the outer canthi of both eyes. Data were filtered on-line with a band-pass of 0.1 to 50 Hz. The signal was digitized with a 16-bit resolution at a sampling rate of 254.31 Hz.

Data analysis

All continuous MEG records were off-line filtered with a finite impulse response band-pass filter: 1997 points, corner frequencies (−3 dB) of 1.1 Hz to 19.9 Hz. This filter provided strong DC suppression (−80 dB; 0.0–0.5 Hz range) to allow for averaging without baseline correction. Trial-based epochs exceeding 100 μV (EOG) or 1100 fT (MEG) standard deviation within a sliding

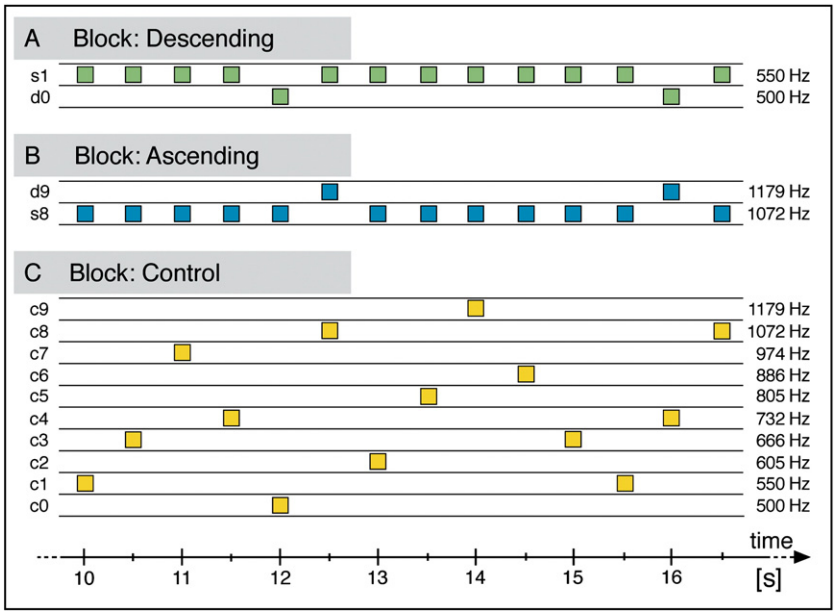

Fig. 1. Experimental design. Stimuli were presented block wise. Three types of blocks existed: (A) descending deviants (10%) amongst low sound frequency standards, (B) ascending deviants (10%) among high sound frequency standards and (C) controls. The squares symbolize a single tone. The width of the square does not match the actual duration of 50 ms. The distance between squares matches the stimulus onset-to-onset interval.

200 ms window were excluded from further analysis. Blocks showing head movement exceeding 8 mm were excluded. Event-related fields (ERF) of 500 ms duration (−100 to 400 ms relative to stimulus onset) were computed separately for each condition, block and participant. In particular, ERFs were derived for both deviants (500 Hz [d0], 1179 Hz [d9]), both standards (550 Hz [s1], 1072 Hz [s8]) and four controls (c0, c1, c8, c9). Block-based ERFs underwent a transformation of sensor positions to individual participants' average head positions across sessions and blocks (Knösche, 2002). Transformed ERFs were aggregated across sessions and blocks for each participant and condition.

Individual event-related field differences (ERF differences) were computed separately for the lower and the higher frequency ranges for the following subtractions. Same-stimulus contrasts were derived for deviant-minus-control (D − C) and standard-minus-control (S − C) subtractions. Different stimulus contrasts were derived for the traditional deviant-minus-standard (D − S) subtractions.

Centered root mean square (RMS) signals were computed separately for both hemispheres as the square root of the mean squared deviations from the spatial mean signal, i.e., the spatial standard deviation for each sample, separately for each hemisphere including 64 MEG channels from either side, thereby omitting 20 channels above the midline (cf. Fig. 2).

Principal component analysis

Spatial PCA was used to reduce the dimensionality of the 148-channel ERFs. It was computed on the level of the individual D − C, D − S and S − C difference fields using the time window between 0 and 300 ms relative to stimulus onset. This window contained a sufficient number of data points, clearly included the N1 difference effect and the MMN, while not extending to time intervals irrelevant for the present hypotheses. The first factor was used for the assessment of N1 and MMN effects. In case the first factor did not show a clear double-bipolar field distribution, the individual factor was selected on the basis of distinct dipolar patterns estimated from the second PCA factor. Latencies of maximal activity determined from factor time courses and eigenvalues of the selected factors were analyzed. Values were submitted to a repeated measures analyses of variance (ANOVA) for the N1 with the factors sound frequency (low, high) and condition (D − C, S − C) and for the MMN with the factors sound frequency (low, high) and condition (D − C, D − S).

Moving dipole computation

Volume conductor models were generated on the basis of individual T1-weighted MRIs. Inner-skull-surface one-shell models were tessellated using 7-mm typical grid length. One equivalent current dipole per hemisphere was computed for each participant, condition and sample point in an N1 (105–125 ms) and an MMN (170–200 ms) time window using seed points in the auditory cortices. Time windows were established based on peak latencies and variance of the grand-average root-mean-square signals. Goodness-of-fit values of the two-moving-dipoles model comprising all 148 MEG channels had to exceed a threshold of 83%. Dipole locations had to be more lateral than 35 mm relative to the interhemispheric sagittal plane. Individual dipole locations were transformed to Talairach coordinates. Dipole coordinates were averaged separately for each participant, sound frequency (high, low), time window (N1, MMN) and condition (D − C, D − S, S − C).

Results

The results are presented in three parts. First, the time courses and topographic maps of the ERFs as well as additional time domain analyses of all deviance and control contrasts are presented. Then, the PCA results are reported. Finally, moving dipole localizations and spatial effects are reported.

Event-related fields and time domains

Fifteen percent of the measurement blocks had to be excluded from further analysis due to head movements exceeding the 8-mm threshold. All remaining 15 participants had contributed at least 6 blocks. On average, about 15% of all measured epochs were rejected.

Grand-average ERF differences were computed separately for lower and higher sound frequency ranges and the three investigated effects: deviant-minus-standard (D − S: red), standard-minus-control (S − C: blue) and deviant-minus-control (D − C: green); see Figs. 2A and B. For both frequency ranges, the deviance-related waveforms revealed magnetic MMN. The traditional deviant-minus-standard comparisons revealed, as predicted, the strongest and temporally monophasic field deflections. There was a spatially dipolar distribution of the ERF differences. The controlled deviant-minus-control contrast, on the other, showed a temporally biphasic pattern of the waveform, also as expected. Here, the N1 effect was going in the opposite direction than the MMN. Therefore, the controlled MMN could not be due to afferent neural processes leading to the N1, it was necessarily due to separate processes. As in the EEG data, the traditional comparisons showed stronger signals and shorter peak latencies than the controlled comparisons, indicating that the traditional MMNm is comprised of an N1 effect and the genuine MMN. Furthermore, the standard-minus-control contrast also revealed temporally monophasic deflections, reflecting mere N1 effects in spatially dipolar patterns for both hemispheres.

The time courses in most of the temporal channels corresponded nicely to the previously observed time courses of the EEG experiment (Jacobsen and Schröger, 2001). As one can see from the close-ups at both sides, the lower pitch (Fig. 2A) and the higher pitch (Fig. 2B) have produced very similar time courses. Furthermore, within the earlier time window (105–125 ms) only differences against the control show large responses. The picture is different in the later time window (170–200 ms) were the strongest responses were observed for differences involving the deviant.

The topographic maps suggest that the activity stemmed from temporal areas bilaterally. All maps showed a dipolar field distribution equally over both hemispheres. The strongest field deflections were observed over temporal regions bilaterally,

Fig. 2. Grand-average ERF differences for the subtraction contrasts D − C, D − S and S − C, separately for the lower (A) and higher (B) sound frequency ranges. The middle columns show the ERF signals for all 148 sensors. Top of the outer columns display sensors A96 and A111 in a larger scale. For all signals, D − C is in green, D − S in red and S − C in blue. Maps show averaged field distributions of all three differences, the left columns show for the N1 time range (105–125 ms) and the right columns for the MMN time range (170–200 ms).

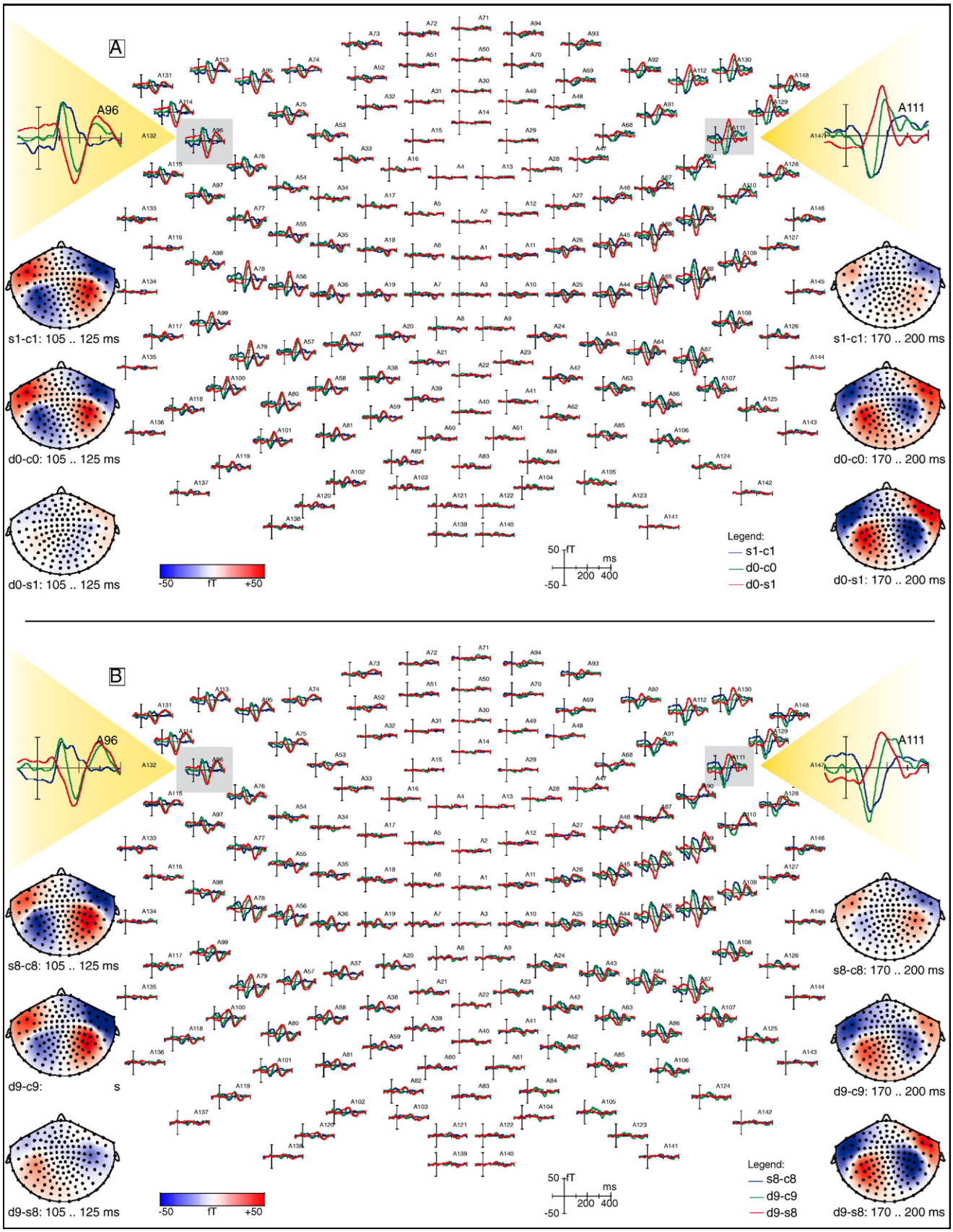
A
A96
A111
s1-c1: 105 .. 125 ms
d0-c0: 105 .. 125 ms
d0-s1: 105 .. 125 ms
-50 fT +50
50 fT
-50
ms
200 400
Legend:
s1-c1
d0-c0
d0-s1
s1-c1: 170 .. 200 ms
d0-c0: 170 .. 200 ms
d0-s1: 170 .. 200 ms
B
A96
A111
s8-c8: 105 .. 125 ms
d9-c9:
s
d9-s8: 105 .. 125 ms
-50 fT +50
50 fT
-50
ms
200 400
Legend:
s8-c8
d9-c9
d9-s8
s8-c8: 170 .. 200 ms
d9-c9: 170 .. 200 ms
d9-s8: 170 .. 200 ms

whereas there was virtually no field change along the midline. Also, the steepest field gradients were at sensor locations over temporal areas. In the MMN time range, deviant-minus-standard and deviant-minus-control showed field distributions that would correspond to a negativity in an EEG measure. The topographic maps at both sides looked all very similar. There is one map or one difference between conditions in each time window which is rather low in amplitude. Note the inverted field deflections for the deviant-minus-control and the standard-minus-control contrasts in the N1 time range (Fig. 2, left columns, panels A and B). The displayed effects are N1 amplitude variations due to a lesser degree of refractoriness in the control condition compared to the other two conditions. Note that, unlike D−S and D−C, the S−C did not reveal the inversion in the MMN time range relative to the N1 time range. This is due to the absence of a mismatch response in the S−C contrast.

Grand-average centered root mean square (RMS) signals derived from the ERF differences are shown in Fig. 3; left column left hemisphere; right column right hemisphere. Signal traces are proportional to the magnetic field strength measured either in all left or right sensors of the whole-head system. For both frequency ranges, the biphasic nature of the controlled MMN contrast was represented by double peaks in the grand-average RMS signals. Both these peaks were virtually traced by one and only one of the other contrasts. The standard-minus-control curve traced the first peak representing the N1 effect. The second peak was mated in time course by the traditional deviant-minus-standard contrast.

The RMS signals were computed to allow for statistical analysis based on the measured magnetic field strength. Because RMS signals are computed via sums of squares negative deflections do not exist. Instead of 148 MEG signals only two RMS signals, one per hemisphere, were taken into account for the statistics. Same time windows as for the dipole analysis were used because they covered the strongest activity of N100 and MMN effects. These figures visualize the time courses of all three evoked difference effects in a much more comprised way than the complete sensor layout of Fig. 2.

One ANOVA was computed for the earlier time window (N1: 105–125 ms) and the differences standard-minus-control and deviant-minus-control. A second ANOVA was conducted testing values from the later time window (MMN: 170–200 ms) taken from the differences deviant-minus-standard and deviant-minus-control. Both ANOVAs were organized as three-way ANOVAs with the factors COND (see above), PITCH (high and low) and HEM (left and right). For the N1 window data from only 14 out of the 15 subjects were used. One participant showed no N1 in one condition and a very weak N1 response in the other critical condition. There was a significant two-way interaction PITCH × HEM for the N1 window $F(1,13)=8.38$, $p=0.013$. There was also a main effect for HEM, which was not further interpreted here, as it could be explained by head positions which were not centered but more to the right within the Dewar. The second time window did not yield any statistical differences.

Principal component analysis

An example for the PCA results presentation of one subject (condition: deviant-minus-standard, lower pitch) is displayed in

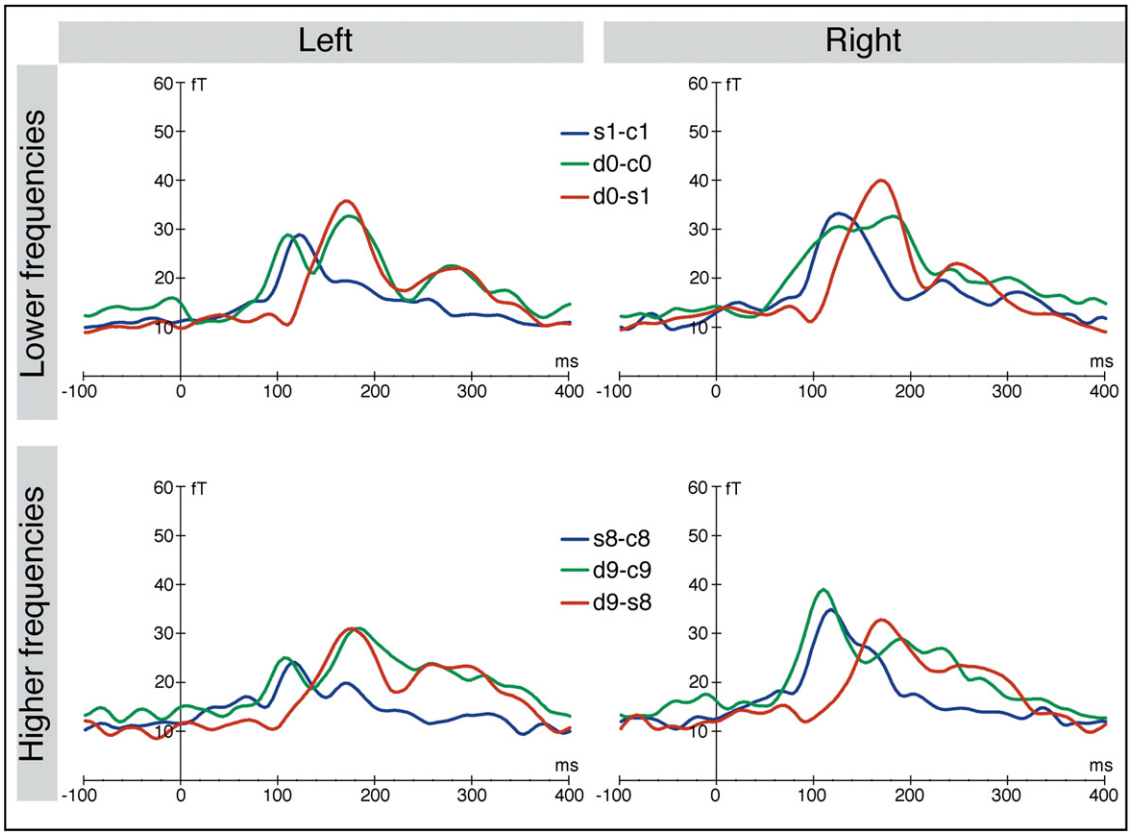

Fig. 3. Grand-average root mean square signals estimated for the two hemispheres and the two sound frequency ranges separately. Color coding is identical to Fig. 2.

Fig. 4. The upper left corner of Fig. 4 contains a logarithmic plot of the six largest eigenvalues. The eigenvalues are given as relative values in respect to the determined noise level leading to a signal-to-noise-ratio (SNR) scaling. Signals plotted in the upper right corner of Fig. 4 are the root of the sum of squared signals (RMS) also in SNR scaling. The upper curve displays the full time range available from the loaded file, the lower right curves focus on the time range being analyzed by the spatial PCA starting with the onset of the tone (0 ms) and lasting for 300 ms. The lower part of Fig. 4 contains the spatial distributions (left column) and the time courses (right column) of the five largest PCA factors.

In about 90% of the analyses the first factor was meaningful in the sense that the spatial distribution could be explained by two temporal dipoles placed at either hemisphere and oriented inferiorly which would have produced a negative deflection in an EEG study. The PCA transformation can be used to map the 148-channel data onto a single virtual channel. In contrast to the RMS analysis, the PCA provides spatial and polarity information in addition to the temporal activity pattern.

For the N1 effects, two separate two-way ANOVAs were computed for the loadings and for the latencies. The factors PITCH (high, low) and COND (deviant-minus-control, standard-minus-control) were investigated. There was no significant effect for the loadings. For the latencies we found two main effects-higher pitches elicited earlier maxima $F(1,13)=6.58$, $p<0.05$ and the maximum of the difference deviant-minus-control is significantly earlier then the one of standard-minus-control $F(1,13)=20.75$, $p<0.001$ within the N1 window.

For the MMN effects, two separate two-way ANOVAs were conducted considering the same factors PITCH and COND. Here, the conditions deviant-minus-control and deviant-minus-standard were tested. There was a significant main effect for COND in both

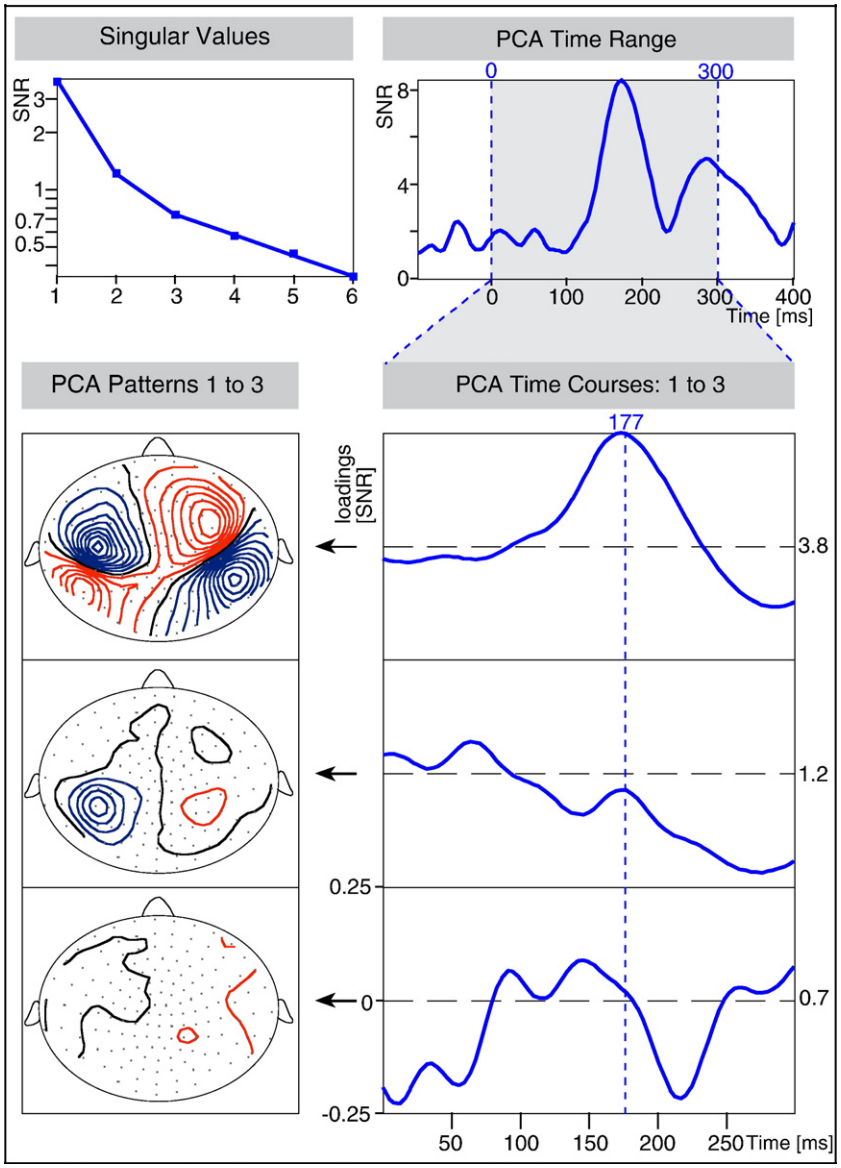

Fig. 4. PCA of a single subject (deviant minus standard, lower pitch). In the upper left corner the eigenvalues of the PCA are plotted on a logarithmic scale. Just one factor seems to be significantly larger than one. The first factor showed a rather classical bi-dipolar field distribution. The most prominent activity is at 177 ms. This latency was taken as optimal for the dipole fits because the strength of the other factors is almost minimal here.

ANOVAs. In case of loadings it resulted in $F(1,14)=6.47$, $p<0.05$ demonstrating that deviant-minus-control elicited smaller effects than deviant-minus-standard. For the latencies, it revealed that deviant-minus-control had a later amplitude maximum than deviant-minus-standard, $F(1,14)=10.21$, $p<0.01$.

Moving dipoles

There were 595 dipole positions for the MMN time window. Maximally, 840 positions could have been obtained (15 participants × 2 conditions × 2 pitch × 2 hem × 7 samples), which yields a rate of 71% of successfully located dipoles. There were 366 dipole positions for the N1 time window. A maximum of 560 could have been obtained (14 subjects × 2 conditions × 2 pitch × 2 hem × 5 samples), which was a rate of 65%. In preparation for the ANOVA, mean dipole positions per subject, condition, hemisphere, pitch and window were computed. Due to the averaging across time windows, the rate of successfully estimated dipole positions was found to be typically 80% and never less than 70% in each cell. Mean positions, which could not be estimated due to the lack of positions (no dipole was observed within the interval under consideration), were replaced by the sum of the mean dipole position estimated across all subjects for the corresponding condition, hemisphere, pitch, window and the individual mean deviation from the overall mean dipole position. Statistical analyses of mean dipole locations yielded qualitatively identical results when the latter individual correction for subjects was not applied.

For both sound frequency ranges, Fig. 5 gives grand-average, and individual dipole localizations, separately for the N1 (left panel) and MMN times ranges (right panel). Grand-average dipole locations are shown superimposed on structural MRIs of an individual participant's brain scaled to Talairach coordinates. Taking a margin of error of 10 mm into consideration, dipoles localized to the gyrus temporales transversus, the so-called Heschl's gyrus, bilaterally.

Table 1 gives the Talairach coordinates of the grand-average moving dipole locations for all conditions. Separate two-way ANOVAs (COND × PITCH) were conducted for each time window, hemisphere and dipole position coordinate (x, y, z) resulting in 12 tests. There was a significant main effect for the z-coordinate in the right hemisphere and the N1 time window in factor COND: $F(1,13)=4.70$, $p=0.05$. These results indicate that in the right hemisphere activity of condition deviant-minus-control was located more inferior (about 4 mm) to activity of condition standard-minus-control.

While investigating the MMN time window a COND × PITCH interaction was found for the y-coordinate of the right hemisphere: $F(1,14)=5.85$, $p=0.03$. Analyzing the means it displayed a difference for condition deviant-minus-control between high and low pitch. (Most parietal was deviant-minus-control high pitch,

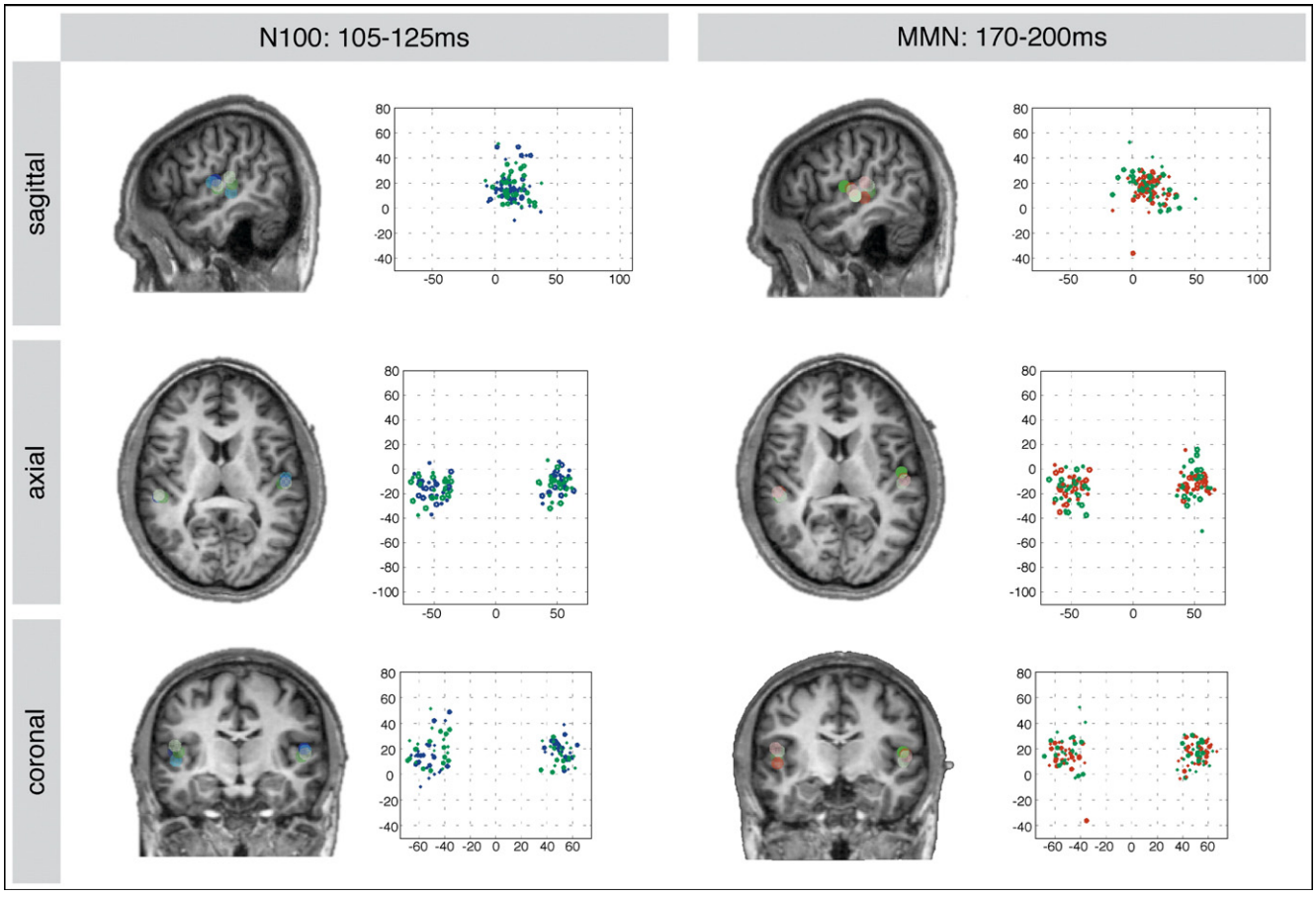

Fig. 5. Average dipole localizations for two conditions and for two sound frequency ranges in the N1 and MMN time ranges. Mean and individual locations of differences between deviants and standards are displayed in red, of differences between deviants and controls in green and finally differences between standards and controls are visualized in blue. Graded reductions in brightness of the colors reflect distance from the displayed slice (partially transparent brain).

Table 1

		x	y	z
N1—left				
C−S	Hi	−51	−16	11
	Lo	−53	−16	18
D−C	Hi	−51	−14	23
	Lo	−49	−16	18
N1—right				
C−S	Hi	52	−9	18
	Lo	51	−11	20
D−C	Hi	52	−13	15
	Lo	49	−13	13
MMN—left				
D−C	Hi	−49	−17	20
	Lo	−51	−18	16
D−S	Hi	−52	−16	17
	Lo	−50	−14	11
MMN—right				
D−C	Hi	50	−15	12
	Lo	50	−6	19
D−S	Hi	50	−10	15
	Lo	52	−12	17

most frontal was deviant-minus-control, low pitch and in the middle there were both pitches of deviant-minus-standard.) A main effect were found for PITCH and the *z*-coordinate of the right hemisphere: $F(1,14)=6.13$, $p=0.03$. In the right hemisphere, higher pitch elicited activity at a more inferior location than the lower pitch.

Finally, we compared the dipole locations from the N1 time window and condition 'S−C' with locations from the MMN time window and condition 'D−C' as a test for different locations between the refractory part of the N1 and the 'cognitive portion' of the MMNm by further six ANOVAs for each hemisphere and coordinate separately. There was only one main effect of PITCH for the *z*-coordinate of the right hemisphere: $F(1,13)=8.89$, $p=0.01$. Higher sound frequencies were located more inferior than lower frequencies.

Discussion

MEG and a controlled experimental protocol were used to investigate the temporal and spatial characteristics of the MMNm to changes in pitch. Participants ignored infrequently occurring deviant sounds that were unpredictably interspersed among frequently presented standard sounds. In addition to this classic oddball sequence, a blocked control condition was employed in which multiple sounds, including the deviant and standard sounds from the oddball block, occurred with equal probability. The latter was identical to the probability of occurrence of the deviant in the oddball block. As in the forerunner EEG study (Jacobsen and Schröger, 2001), two frequency ranges were investigated, allowing for an internal assessment of reliability.

The MEG waveforms displayed magnetic MMN for both frequency ranges, as predicted. The traditional deviant-minus-standard comparisons revealed temporally monophasic effects with dipolar distributions of the event-related difference fields that would each correspond to a negativity in an EEG measure. In contrast, the temporally biphasic patterns of the waveforms in the controlled MMN contrasts indicated reversed N1 effects. As a consequence, this effect could not be due to afferent neural processes leading to the N1, it must be due to separate processes. Moreover, the traditional deviant-minus-standard comparisons showed stronger signals and shorter peak latencies than the controlled comparisons, indicating that the traditional MMNm is comprised of an N1 effect and the genuine MMN.

Given the assumption that EEG and MEG measures are adequately comparable (Huotilainen et al., 1998), the MEG showed numerous similarities with our previously reported EEG data reflecting the detection of changes in pitch (Jacobsen and Schröger, 2001; Jacobsen et al., 2003b). The genuine MMN derived from the Controlled Protocol had a temporally biphasic pattern. The traditional comparisons were temporally monophasic and showed stronger signals and shorter peak latencies than the controlled comparisons. Time courses of the former effects were highly comparable (cf. Jacobsen and Schröger, 2001). Up to this level of analysis, the present pattern of MEG results constitutes a complete replication of the earlier ERP data.

The spatiotemporal patterns of ERF differences showed clear dipolar distribution over both hemispheres in the present data. However, grand-average ERFs are not optimal for source localizations (Lütkenhöner, 2003), as the MEG sensor array does not scale with individual subject's head size, as EEG electrode placements do. Consequently, estimates of neural source localizations were based on individual data sets in the present study. The centered root mean square (RMS) data aggregated the ERFs into one channel per hemisphere, thus reducing the spatial information while maintaining the temporal information. For both frequency ranges, the biphasic nature of the controlled MMN contrast is represented by double peaks in the grand-average RMS signals. Both these peaks are virtually traced by one and only one of the other contrasts. The standard-minus-control curve traces the first peak representing the N1 effect. The second peak is matched in time course by the traditional deviant-minus-standard contrast.

In contrast to an RMS transformation, the principal component analysis computation conserves polarity information. The PCA ANOVA clearly showed that the traditional deviant-minus-standard contrast was partly due to refractory effects. It leads to a stronger signal and an earlier peaking activity representing N1 effects and MMN.

Individual moving dipoles were successfully identified in the N1 time window for the differences deviant-minus-standard and standard-minus-control as well as in the MMN time window for the differences deviant-minus-control and deviant-minus-standard. Taking a margin of error of 10 mm into consideration, group mean of dipoles localized to the gyrus temporales transversus, or Heschl's gyrus, bilaterally. There were four significant condition effects on dipole locations when no corrections for multiple tests were applied. However, due to the multiple comparison nature of the significance testing of the dipole locations, a correction procedure, like Bonferroni, is adequate. This procedure rendered all effects non significant. As a consequence, the present approach of individual moving dipole localizations did not yield a separation of non-comparator (N1 time window) and comparator (MMN time window) contributions to the deviance-related brain responses. Based on previous studies reporting a spatial separation of N1 proper and MMN sources, a comparable effect could have been expected for the present comparator and non-comparator contrasts

(e.g., Alho et al., 1993; Korzyukov et al., 2003; Rinne et al., 2000; Tiitinen et al., 1993; for a review, see Alho, 1995). This shows that possible spatial differences between frequency-specific N1 subcomponents and the MMN sources have to be rather small resulting in non-significant effects (cf. Näätänen and Picton, 1987).

In the current debate about the nature of MMN (Jääskeläinen et al., 2004; Näätänen et al., 2005), the present data also yielded corroborating evidence for the memory-based comparison account of MMN generation. The controlled MMN of the deviant-minus-control contrast showed an inverted field deflection in the N1 time range due to N1 refractory processes, as compared to the MMN (see Fig. 2 deviant-minus-control (D − C) maps in the left columns of panels a and b). Additionally, the RMS plots revealed this data pattern, in an analysis that focuses on aggregated signal strength regardless of polarity. We assume, that refractoriness effect observed even for deviants can be explained by the close neighborhood in sound frequency to the standards. In other words, due to a partial overlap in tonotopic neurons repeating the standard tones causes activity in neurons that are also responsive to the deviants. This happens, of course, also when presenting the controls, but here the effect is reduced because the neighboring controls occur only in 10% of the trials while standards occur in 90% of the trials. Deviance detection, as reflected by effects on the N1, is sensorial in nature and is based on a non-comparator mechanism of automatic change detection (cf. Siddle, 1991), whereas the genuine MMN reflects cognitive processing involving a comparator mechanisms using auditory sensory memory representations (for additional evidence for the memory-based account of the MMN, see Näätänen et al., 2005).

Conclusion

Taken together, the present MEG data provide a strong indication for the existence of temporally distinct but spatially overlapping activities of non-comparator-based and comparator-based mechanisms of automatic frequency change detection in auditory cortex. The genuine MMNm to changes in sound frequency reflects the detection of auditory deviance-based sensory memory representations. Automatic frequency change detection in auditory cortex based on differential states of neural refractory states takes place prior to the comparator-based processes but cannot provide an alternative interpretation of the MMN.

Acknowledgments

The present work was partly supported by the DFG. The authors wish to thank Yvonne Wolff for carefully conducting the MEG recording.

References

Alho, K., 1995. Cerebral generators of mismatch negativity (MMN) and its magnetic counterpart (MMNm) elicited by sound changes. Ear Hear. 16, 38–51.

Alho, K., Huotilainen, M., Tiitinen, H., Ilmoniemi, R.J., Knuutila, J., Näätänen, R., 1993. Memory-related processing of complex sound patterns in human auditory cortex: a MEG study. NeuroReport 4, 391–394.

Butler, R.A., Spreng, M., Keidel, W.D., 1969. Stimulus repetition rate factors which influence the auditory potential in man. Psychophysiology 5, 665–672.

Fischer, C., Morlet, D., Bouchet, P., Luaute, J., Jourdan, C., Salord, F., 1999. Mismatch negativity and late auditory evoked potentials in comatose patients. Clin. Neurophysiol. 110, 1601–1610.

Huotilainen, M., Winkler, I., Alho, K., Escera, C., Virtanen, J., Ilmoniemi, R.J., Jääskeläinen, I.P., Pekkonen, E., Näätänen, R., 1998. Combined mapping of human auditory EEG and MEG responses. Electroencephalogr. Clin. Neurophysiol. 108, 370–379.

Huotilainen, M., Kujala, A., Hotakainen, M., Parkkonen, L., Taulu, S., Simola, J., Nenonen, J., Karjalainen, M., Näätänen, R., 2005. Short-term memory functions of the human fetus recorded with magnetoencephalography. NeuroReport 16, 81–84.

Jääskeläinen, I.P., Ahveninen, J., Bonmassar, G., Dale, A.M., Ilmoniemi, R.J., Levänen, S., Lin, F.-H., May, P., Melcher, J., Stufflebeam, S., Tiitinen, H., Belliveau, J.W., 2004. Human posterior auditory cortex gates novel sounds to consciousness. Proc. Natl. Acad. Sci. U. S. A. 17, 6809–6814.

Jacobsen, T., Schröger, E., 2001. Is there pre-attentive memory-based comparison of pitch? Psychophysiology 38, 723–727.

Jacobsen, T., Schröger, E., 2003. Measuring duration mismatch negativity. Clin. Neurophysiol. 114, 1133–1143.

Jacobsen, T., Horenkamp, T., Schröger, E., 2003a. Pre-attentive memory-based comparison of sound intensity. Audiol. Neuro-Otol. 8, 338–346.

Jacobsen, T., Schröger, E., Horenkamp, T., Winkler, I., 2003b. Mismatch negativity to pitch change: varied stimulus proportions in controlling effects of neural refractoriness on human auditory event-related brain potentials. Neurosci. Lett. 344, 79–82.

Knösche, T.R., 2002. Transformation of whole head MEG recordings between different sensor positions. Biomed. Tech. 47, 59–62.

Korzyukov, O.A., Winkler, I., Gumenyuk, V.I., Alho, K., 2003. Processing abstract auditory features in the human auditory cortex. NeuroImage 20, 2245–2258.

Kujala, T., Tervaniemi, M., Schröger, E., 2007. The mismatch negativity in cognitive and clinical neuroscience: theoretical and methodological considerations. Biol. Psychol. 74, 1–19.

Lütkenhöner, B., 2003. Single-dipole analyses of the N100m are not suitable for characterizing the cortical representation of pitch. Audiol. Neuro-otol. 8, 222–233.

Näätänen, R., 1992. Attention and Brain Function. Erlbaum, Hillsdale, NJ.

Näätänen, R., Alho, K., 1997. Higher-order processes in auditory-change detection. Trends Cogn. Sci. 2, 44–45.

Näätänen, R., Picton, T., 1987. The N1 wave of the human electric and magnetic response to sound: a review and an analysis of the component structure. Psychophysiology 24, 375–425.

Näätänen, R., Gaillard, A., Mäntysalo, S., 1978. Early selective attention reinterpreted. Acta Psychol. 42, 313–329.

Näätänen, R., Sams, M., Alho, K., Paavilainen, P., Reinikainen, K., Sokolov, E.N., 1988. Frequency and location specificity of the human vertex N1 wave. Electroencephalogr. Clin. Neurophysiol. 69, 523–531.

Näätänen, R., Paavilainen, P., Alho, K., Reinikainen, K., Sams, M., 1989. Do event-related potentials reveal the mechanism of auditory sensory memory in the human brain? Neurosci. Lett. 98, 217–221.

Näätänen, R., Tervaniemi, M., Sussman, E., Paavilainen, P., Winkler, I., 2001. “Primitive intelligence” in the auditory cortex. Trends Neurosci. 24, 283–288.

Näätänen, R., Jacobsen, T., Winkler, I., 2005. Memory-based or afferent processes in mismatch negativity (MMN): a review of the evidence. Psychophysiology 42, 25–32.

Oldfield, R., 1971. The assessment and analysis of handedness: the Edinburgh Inventory. Neuropsychologia 9, 97–113.

Opitz, B., Schröger, E., von Cramon, D.Y., 2005. Sensory and cognitive mechanisms for preattentive change detection in auditory cortex. Eur. J. Neurosci. 21, 531–535.

Paavilainen, P., Alho, K., Reinikainen, K., Sams, M., Näätänen, R., 1991. Right hemisphere dominance of different mismatch negativities. Electroencephalogr. Clin. Neurophysiol. 78, 466–479.

Pantev, C., Hoke, M., Lehnertz, K., Lütkenhöner, B., Anogianakis, G., Wittkowski, W., 1988. Tonotopic organization of the human auditory

cortex revealed by transient auditory evoked magnetic fields. Electroencephalogr. Clin. Neurophysiol. 69 (2), 160–170.

Pekkonen, E., Hirvonen, J., Jääskeläinen, I.P., Kaakkola, S., Huttunen, J., 2001. Auditory sensory memory and the cholinergic system: implications for Alzheimer's disease. NeuroImage 14, 376–382.

Picton, T.W., Woods, D.L., Proulx, G.B., 1978. Human auditory sustained potentials: II. Stimulus relationships. Electroencephalogr. Clin. Neurophysiol. 45, 198–210.

Rinne, T., Alho, K., Ilmoniemi, R.J., Virtanen, J., Näätänen, R., 2000. Separate time behaviors of the temporal and frontal mismatch negativity sources. NeuroImage 12, 14–19.

Ritter, W., Vaughan, H.G., Costa, L.D., 1968. Orienting and habituation to auditory stimuli: a study of short term changes in average evoked responses. Electroencephalogr. Clin. Neurophysiol. 25, 550–556.

Romani, G.L., Williamson, S.J., Kaufman, L., 1982. Tonotopic organization of the human auditory cortex. Science 216 (4552), 1339–1340.

Schröger, E., 1997. Higher-order processes in auditory-change detection: a response to Näätänen and Alho. Trends Cogn. Sci. 2, 45–46.

Schröger, E., Wolff, C., 1996. Mismatch response to changes in sound location. NeuroReport 7, 3005–3008.

Siddle, D.A., 1991. Orienting, habituation, and resource allocation: an associative analysis. Psychophysiology 28, 245–259.

Tervaniemi, M., Kujala, A., Alho, K., Virtanen, J., Ilmoniemi, R.J., Näätänen, R., 1999. Functional specialization of the human auditory cortex in processing phonetic and musical sounds: a magnetoencephalographic (MEG) study. NeuroImage 9, 330–336.

Tiitinen, H., Alho, K., Huotilainen, M., Ilmoniemi, R.J., Simola, J., Näätänen, R., 1993. Tonotopic auditory cortex and the magnetoencephalographic (MEG) equivalent of the mismatch negativity. Psychophysiology 30, 537–540.

Weber, C., Hahne, A., Friedrich, M., Friederici, A.D., 2004. Discrimination of word stress in early infant perception: electrophysiological evidence. Cogn. Brain Res. 18, 149–161.

Winkler, I., Reinikainen, K., Näätänen, R., 1993. Event-related brain potentials reflect echoic memory in humans. Percept. Psychophys. 53, 443–449.